



TECHNICAL REPORT RD-AS-01-02

***DESIGN OF A MILLIMETER WAVE DATA
LINK FOR A RADAR GUIDED MISSILE***

Larry J. Levitt

Advanced Systems Directorate
Aviation and Missile Research, Development, and Engineering Center

September 2001

Approved for public release; distribution is unlimited.

DESTRUCTION NOTICE

FOR CLASSIFIED DOCUMENTS, FOLLOW THE PROCEDURES IN DoD 5200.22-M, INDUSTRIAL SECURITY MANUAL, SECTION II-19 OR DoD 5200.1-R, INFORMATION SECURITY PROGRAM REGULATION, CHAPTER IX. FOR UNCLASSIFIED, LIMITED DOCUMENTS, DESTROY BY ANY METHOD THAT WILL PREVENT DISCLOSURE OF CONTENTS OR RECONSTRUCTION OF THE DOCUMENT.

DISCLAIMER

THE FINDINGS IN THIS REPORT ARE NOT TO BE CONSTRUED AS AN OFFICIAL DEPARTMENT OF THE ARMY POSITION UNLESS SO DESIGNATED BY OTHER AUTHORIZED DOCUMENTS.

TRADE NAMES

USE OF TRADE NAMES OR MANUFACTURERS IN THIS REPORT DOES NOT CONSTITUTE AN OFFICIAL ENDORSEMENT OR APPROVAL OF THE USE OF SUCH COMMERCIAL HARDWARE OR SOFTWARE.

REPORT DOCUMENTATION PAGE

Form Approved
OMB No. 074-0188

Public reporting burden for this collection of information is estimated to average 1 hour per response, including the time for reviewing instructions, searching existing data sources, gathering and maintaining the data needed, and completing and reviewing this collection of information. Send comments regarding this burden estimate or any other aspect of this collection of information, including suggestions for reducing this burden to Washington Headquarters Services, Directorate for Information Operations and Reports, 1215 Jefferson Davis Highway, Suite 1204, Arlington, VA 22202-4302, and to the Office of Management and Budget, Paperwork Reduction Project (0704-0188), Washington, DC 20503

1. AGENCY USE ONLY		2. REPORT DATE August 2001		3. REPORT TYPE AND DATES COVERED Final; December 1999 to June 2000	
4. TITLE AND SUBTITLE Design of a Millimeter Wave Data Link for a Radar Guided Missile				5. FUNDING NUMBERS	
6. AUTHOR(S) Larry J. Levitt					
7. PERFORMING ORGANIZATION NAME(S) AND ADDRESS(ES) Commander, U. S. Army Aviation and Missile Command ATTN: AMSAM-RD-AS Redstone Arsenal, AL 35898-5247				8. PERFORMING ORGANIZATION REPORT NUMBER TR-RD-AS-01-02	
9. SPONSORING / MONITORING AGENCY NAME(S) AND ADDRESS(ES)				10. SPONSORING / MONITORING AGENCY REPORT NUMBER	
11. SUPPLEMENTARY NOTES					
12a. DISTRIBUTION / AVAILABILITY STATEMENT Approved for public release; distribution is unlimited.				12b. DISTRIBUTION CODE A	
13. ABSTRACT (Maximum 200 Words) This report describes a systems-level design of a data link that enables a high velocity missile to receive guidance commands from a 35 GHz radar. The objectives for this design include a Bit Error Rate (BER) of 10^{-6} at 1 km downrange, low power consumption, and miniaturized components so that the data link can fit on the back of a missile. No custom designed electronic chips are necessary. The design assumes the implementation of Boolean equations for Cyclic Redundancy Checking (CRC) on a programmable logic device. The report concludes that based on a simple rainfall attenuation model, the system can meet the BER performance objective in moderate rain.					
14. SUBJECT TERMS Bit error Rate (BER); Millimeter Wave Data Link; Radar				15. NUMBER OF PAGES 55	
				16. PRICE CODE	
17. SECURITY CLASSIFICATION OF REPORT UNCLASSIFIED	18. SECURITY CLASSIFICATION OF THIS PAGE UNCLASSIFIED	19. SECURITY CLASSIFICATION OF ABSTRACT UNCLASSIFIED		20. LIMITATION OF ABSTRACT SAR	

NSN 7540-01-280-5500

i/(ii Blank)

Standard Form 298 (Rev. 2-89)
Prescribed by ANSI Std. Z39-18
298-102

ACKNOWLEDGEMENT

The author would like to thank Dr. Brian J. Smith, U. S. Army Aviation and Missile Research, Development, and Engineering Center, U. S. Army Aviation and Missile Command, for suggesting the topic and for guidance throughout the project.

TABLE OF CONTENTS

	<u>Page</u>
I. INTRODUCTION.....	1
II. PROJECT DEFINITION AND BACKGROUND.....	2
III. DESIGN APPROACH.....	3
IV. DESIGN ANALYSIS.....	5
A. Radar Range Equation	5
B. Modulation Technique.....	6
C. Antenna Gain.....	8
D. Error Control Technique	9
V. DESIGN PRESENTATION.....	10
VI. ATMOSPHERIC EFFECTS ON COMMUNICATION SYSTEMS.....	12
A. Attenuation By Clear Air	12
B. Attenuation By Rainfall.....	12
C. Attenuation By Clouds, Fog, and Smoke	16
D. Attenuation By Frozen Hydrometeors	16
E. Design Implications.....	17
VII. CONCLUSION	19
REFERENCES.....	21
BIBLIOGRAPHY	25
APPENDIX A: MARKET RESEARCH.....	A-1
APPENDIX B: PATENT SEARCH	B-1
APPENDIX C: LOGARITHMIC FORM OF THE RADAR RANGE EQUATION.....	C-1
APPENDIX D: BIT ERROR RATE VERSUS RANGE FOR 4, 16, AND 64 QAM.....	D-1
APPENDIX E: QAM DEMODULATOR.....	E-1

TABLE OF CONTENTS

	<u>Page</u>
APPENDIX F: DIGITAL DOWN CONVERTER	F-1
APPENDIX G: REFERENCE LIST	G-1

LIST OF ILLUSTRATIONS

<u>Figure</u>	<u>Title</u>	<u>Page</u>
1.	RF Receiver Systems	4
2.	SNR (dB) Versus Range to Target (m). Transmit Power = 750 MW, $G_t = 49$ dB	6
3.	BER Versus Range to Target (m). Transmit Power = 750 MW, $G_t = 49$ dB	7
4.	BER Versus Range to Target (m). Transmit Power = 750 MW, $G_t = 65$ dB.....	8
5.	Digital MMW Receiver Design. Numbers Refer to Parts Listing	9
6.	Effect of Rainfall Attenuation on BER Versus Range to Target	10

LIST OF TABLES

<u>Table</u>	<u>Title</u>	<u>Page</u>
1.	Antenna Gain Based on Aperture Area ($\rho_a = 0.5$, $\lambda = 0.0086\text{m}$)	5
2.	Parts Listing for Millimeter wave Data Link.....	11
3.	Improvements to CCIR – 1986 (31:915-917).....	14
4.	Summary of Rain and Rain Attenuation Models (30:3-2).....	15
5.	Attenuation (α : dB/km) Due to Fog	16
6.	Attenuation (α : dB/km) Due to Snow, Ice Crystals, and Hail.....	17

I. INTRODUCTION

Millimeter Wave (MMW) technology is attractive for systems designers because of the wide bandwidth it offers for data transmission [1]. Another reason is that since the size of the antenna is inversely related to the transmission frequency, small antennas can be utilized. While there are many advantages to using the MMW spectrum (the frequency range of 30 to 300 GHz), lack of adequate power sources prevented its widespread use until recently. Hybrid and Monolithic Millimeter Wave Integrated Circuit (MMIC) techniques emerged in the mid-80s for commercial automotive applications such as collision avoidance radar, industrial sensors to control processes, communications, remote sensing, and many other applications [2].

An important propagation characteristic for MMW radio signals is that they generally travel only a few miles and penetrate solid materials rather poorly. However, MMW can be used for very efficient spectrum utilization, with Low Probability of Intercept/Low Probability of Detection (LPI/LPD) for very secure communications. The choice of MMW is appropriate for this application, since the radar would be transmitting guidance commands by Line-of-Sight (LOS) to a missile equipped with this receiver for a range of no more than 2 km.

It is envisioned that the missile will be used for ground-to-ground applications up to 5 km, such as defeating enemy armored vehicles (assume that another guidance system takes over after 2 km). The narrow beam width reduces multipath effects, which is important since the missile flies relatively close to the ground. For this reason, MMW is considered to be the most accurate choice for low angle tracking [3].

Currently, systems designers are often choosing carrier transmission systems instead of baseband transmission systems. In addition to antenna size considerations, a modulated carrier can carry a complex spectrum, which means that only half the bandwidth is required to carry the data. Also, a modulated carrier can be upconverted (shifted in frequency) if multiple channels are required.

Finally, it is important to note that receiver architectures are being designed with an increasing number of digital components. For example, digital upconverters have been proposed that can replace analog mixers, oscillators, and filters [4]. According to Pentek, Inc., a "digital receiver chip" contains a digital mixer, digital local oscillator, and a decimating low pass filter [5]. Therefore, a digital down converter that performs these functions was included in the final design. Keeping abreast of the latest developments in digital electronics related to signal processing was crucial to the success of this project.

II. PROJECT DEFINITION/BACKGROUND

This project is based on the U. S. Army's need for a short range (~ 5 km) ground-to-ground missile for defeating enemy targets such as armored vehicles. The objective is a systems-level design of an MMW receiver (data link) that enables a high velocity missile to receive guidance commands from a radar operating at 35 GHz (Ka band). As this is a feasibility study, no hardware will be built or tested. The receiver will be a module that can fit on the back of a missile.

The U. S. Army would like to have a prototype within the next 2 to 4 years. If the U. S. Army were to produce a large quantity of missiles (assumed to be 1000 units), the digital MMW receiver should cost \$1000 to \$2000 each. A block diagram of the electronic chips comprising the data link including the cost, vendor name, and part number, can be found in Section V.

The radar transmits a digital data stream one-way to the high velocity missile equipped with this receiver for the first 2 km of its flight. The digital data stream represents commands sent to the guidance computer on the missile, which control the four fins (actuators) on the missile. It is assumed that the fins can rotate ± 5 degrees. The update rate of these commands is 20 MHz [6], that is, once every 50 μ s. The number of bits in the "control word" is 56. This number was arrived at by considering that for each of the 4 fins, 7 bits represent the magnitude of the fin deflection, followed by one sign bit, and 2 bits to identify the appropriate fin (4 fins * 10 bits = 40 bits). An additional 16 bits are appended for error detection.

A complete off-the-shelf package that meets the design objectives of this project is not available (Appendix A). However, "digital receiver chips", which implement Analog-to-Digital (A/D) conversion followed by digital down conversion (digital Radio Frequency (RF) mixer, digital local oscillator, and low pass filter) have been available since the early 90s from companies such as Graychip, Inc. and Harris Corp [5]. A patent search on the term "digital receiver chip" is included in Appendix B.

There is potential for related products, including guidance of unmanned air or ground vehicles, and the ability to communicate with unattended sensors or munitions. Note that as MMW circuits become more commercially available and viable for military use, companies that design MMW products may become more numerous. Hence, competition in this area may increase in the future.

The project objectives (as stated in the project proposal) are:

- BER at 1 km: 10^{-6} or better
- Miniaturized components (chips that occupy mm^2)
- Power consumption as low as possible (preferably MW), but must consider if attenuation by missile plume is significant
- Conform to Federal Communications Commission (FCC) regulations
- Reject frequencies outside the range of interest

- Complete systems diagram, with part number listing (including vendor information and price), if applicable
- Determine whether existing chips or modules may be used, or whether custom-designed chips are necessary

III. DESIGN APPROACH

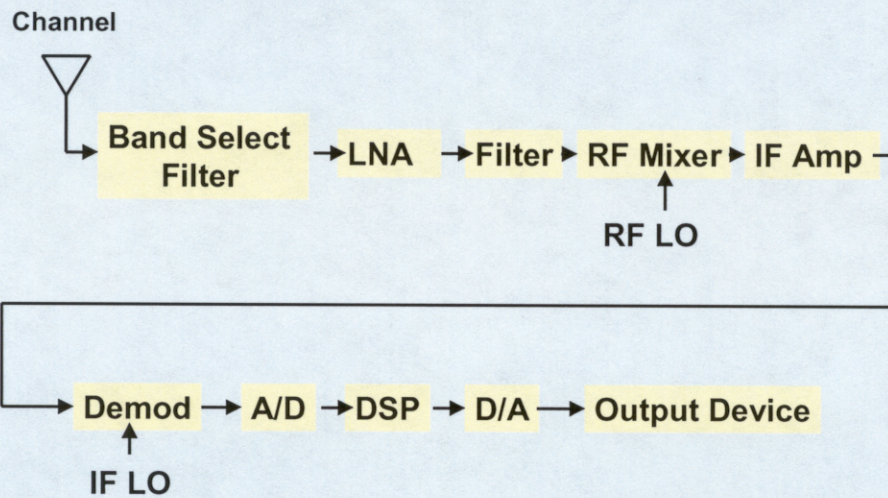
The strategy of the design approach was to develop the design specifications including the choice of modulation scheme, consider the receiver architecture, perform the component search, and recommend the final systems design.

The bandwidth of the radar for this study is 35 GHz (Ka band). It was selected based on atmospheric propagation characteristics (low attenuation), small beam width (reduces multipath for low-angle tracking), and simplicity of components.

The radar range equation [7] was used to compute Signal-to-Noise Ratio (SNR) versus distance downrange for various combinations of transmit power, receiver gain, and transmit gain. A modulation technique was selected based on signal degradation considerations, digital modulation efficiency, and simplicity of implementation. The SNR versus distance downrange computations were converted to BER versus distance downrange based on the choice of modulation technique. This allowed for a determination of the receiver gain for the horn antenna according to the design specifications of a BER of 10^{-6} or better at a distance of 1 km downrange. The effect of rainfall attenuation and attenuation due to the smoke plume of the missile was also considered (Section VI.B). Section IV of this report contains details of the radar range computations.

The receiver architecture was based on the block diagram of an RF communication system (Fig.1). A considerable amount of time was spent on the Digital Signal Processing (DSP) block, since this is where error control techniques for digital communications are placed. Since one or more erroneous bits can cause the missile to be steered off course, an error detection scheme will be included. Due to the high velocity of the missile, particularly the assumed update rate, error correction will not be used, as this requires considerable processing time. Also, error correction would require the design of a transceiver (data link on the missile communicates back to the radar) instead of a receiver (one way communication only), making the overall design much more complicated. Instead of using a simple parity check code (adding a single bit to the message) that can detect only an odd number of errors, a more robust technique known as CRC will be used.

RF Rcvr System Overview



After Stonick, RF Communication Systems, 2000

Figure 1. RF Receiver System

After modifying the receiver architecture for inclusion of a digital down converter, the following components were selected for the final design: horn antenna, band select filter, Low Noise Amplifier (LNA), RF mixer, A/D converter, digital down converter, Quadrature Amplitude Modulation (QAM) chipset for demodulation, and CRC (implemented in a programmable logic device). The output then goes to the missile's guidance computer.

Note that a more in-depth analysis would have to take into account atmospheric noise, system losses due to nonideal components, thermal noise introduced within the radar, and other signal processing losses [7].

IV. DESIGN ANALYSIS

A. Radar Range Equation

Using the radar range equation [7], numerous MATLAB runs were performed to arrive at viable design parameters for the radar/transmitter system. Some additional calculations for the antenna gain based on area of the antenna aperture were performed prior to running the MATLAB program. After starting with unrealistically high values for the transmit power (1 kW), it was found that increasing the antenna gain for both the transmitter and receiver allowed for a reduction in the transmit power to only 750 MW. Specifically, the SNR of 13.4 dB can be achieved with a receiver gain of 35 dB, transmitter gain of 49 dB, and transmit power of 750 MW. Note that SNR ~13 dB is important because it corresponds to a 50 percent probability of false detection for BER of 10^{-6} on the Swerling curves, assuming a known signal in white noise [9].

The bistatic radar equation from Reference 7 for calculating SNR is:

$$\text{SNR} = P_t * G_t * G_r * (\lambda^2) * \sigma / (4 * \pi^3) * (R^4) * k * T * B * F_n * L \quad (1)$$

where P_t is transmitter power (W), G is antenna gain (t:transmitter, r:receiver) in dB, λ is wavelength (m), σ is Radar Cross-Section (m^2), K is Boltzmann's constant, T is temperature (K), B is update rate (MHz), F_n is noise figure (dB), and L is losses (dB). For computational purposes, the logarithmic form of the radar range equation was used (Appendix C), with $\sigma = 5 \text{ m}^2$, $B = 20 \text{ MHz}$, $F_n = 8 \text{ dB}$, and $L = 5 \text{ dB}$ [3, 6, 7, 9].

Using Equation (6-11) from Reference 7, the antenna gain may be calculated from

$$G = 4 * \pi * A * \rho_a / (\lambda^2) \quad (2)$$

where A is the physical area of the aperture and ρ_a is the aperture efficiency (0.5). Table 1 shows antenna gain for various aperture areas.

Table 1. Antenna Gain Based on Aperture Area ($\rho_a = 0.5$, $\lambda = 0.0086\text{m}$)

Area of Antenna Aperture	Antenna Gain (dB)
$(1/16) \text{ in}^2 = (0.000040 \text{ m}^2)$	5.34
$(1/4) \text{ in}^2 = (0.000161 \text{ m}^2)$	13.70
$(1/2) \text{ in}^2 = (0.000322 \text{ m}^2)$	14.38
$1 \text{ in}^2 = (0.000645 \text{ m}^2)$	17.38

Figure 2 depicts SNR versus range to target for receiver gains varying from 20 dB to 35 dB:

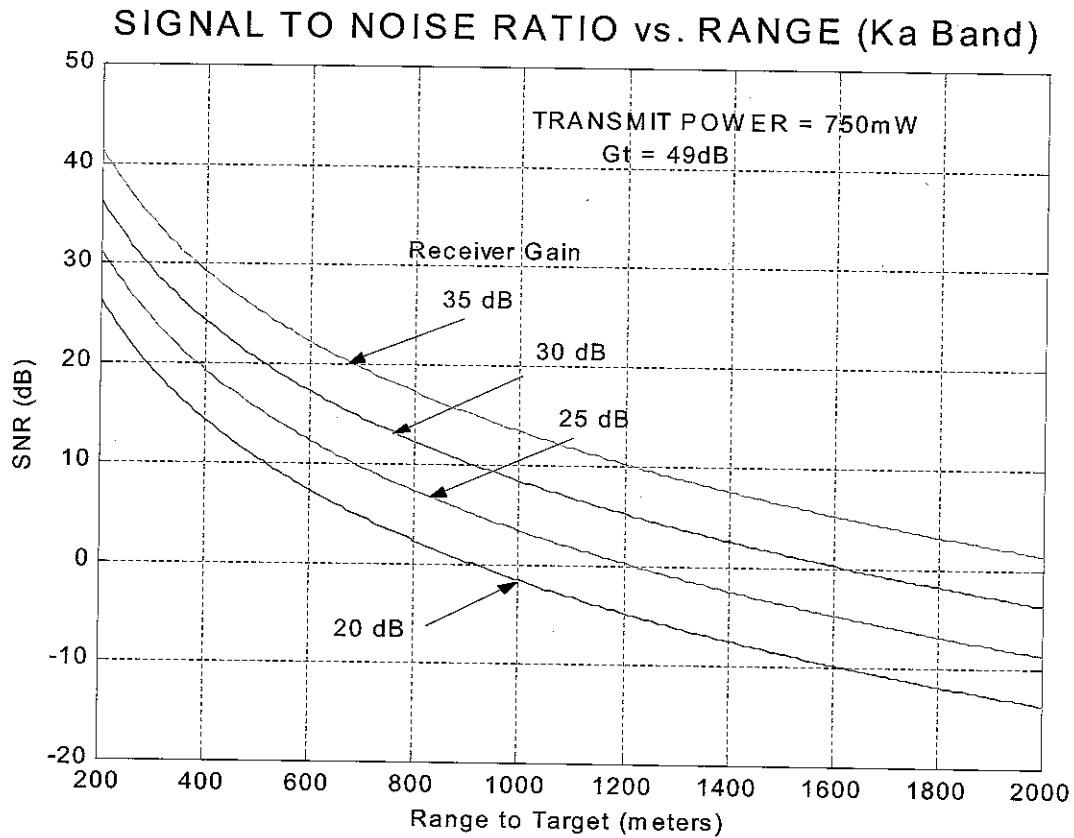


Figure 2. SNR (dB) Versus Range to Target (m). Transmit Power = 750 MW, $G_t = 49\text{ dB}$

B. Modulation Technique

In order to convert the above figure to BER versus range, the modulation scheme must be known. The modulation scheme of choice is QPSK (MQAM with $M=4$), which is typically used in Ka band satellite communications. A comparison of digital M-ary signaling schemes (M-ASK, M-FSK, M-PSK, and QAM) is provided in Table 2.2 of Reference 10. It is shown that QAM is the most efficient technique for multialphabet signaling because it requires the lowest SNR to achieve a given BER when compared with other methods using the same number of states per symbol. Additional data concerning BER versus SNR is provided for these methods [10]. It was emphasized that hardware for QAM is in widespread use and is "rather straightforward".

The BER versus range to target was computed for four different receiver gains. The equation for BER as a function of SNR was taken from Reference 10. This BER approximation is appropriate for coherent Phase Shift Keying (PSK), Minimum Shift Keying (MSK), or Quadriphase Shift Keying (QPSK), assuming a noiseless receiver.

Because of the computational complexity, it is not feasible to perform detailed error probability computations for MPSK, M-Quadrature Amplitude Modulation (QAM), etc. There are numerous algorithms and results that appear in the current literature and textbooks that address this topic [11 through 14]. Although a recent textbook has MATLAB programs for simulated BER, many functions are missing, requiring the estimation of statistical distributions [15]. Note that communications systems designers choose the appropriate modulation method and coding techniques using BER performance. There are many system and channel parameters that affect BER such as SNR, data rate, modulation scheme, and interference from other emitters. Ideally, predictions of Intersymbol Interference (ISI) are useful for justifying the choice of higher order modulation schemes.

The choice of QPSK as a modulation technique allows the DSP portion of the system architecture to be kept simple since QPSK is “not particularly sensitive to ISI”, whereas higher order methods such as 16-QAM and 64-QAM become increasingly sensitive to ISI [16]. This choice allows the ISI to be ignored, because otherwise a Butterworth filter [16] or a channel equalizer such as a Finite Impulse Response (FIR) filter to reduce the ISI [15] would need to be included in the DSP block (Fig. 1). Appendix D shows BER versus range to target for 4 QAM, 16 QAM, and 64 QAM ($G_r = 35$ dB), and Appendix E shows details of the QAM demodulator.

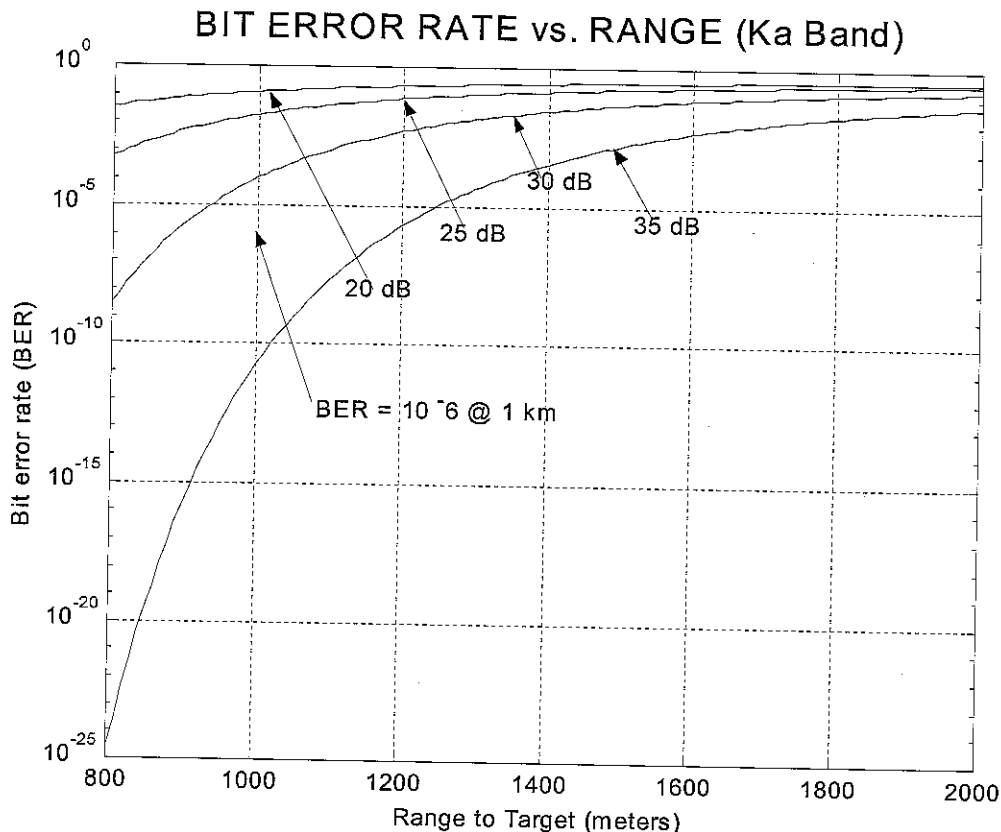


Figure 3. BER Versus Range to Target (m). Transmit Power = 750 MW, $G_t = 49$ dB

C. Antenna Gain

Based on Figure 3, the original design goal for the horn antenna was an antenna gain of 35 dB. However, calculations using Equation (2) indicated that the antenna would be too large to fit on the back of a missile based on the calculated aperture area. Referring back to Table 1, an aperture size approximately 1 inch² was more appropriate. Consequently, a standard gain horn antenna from QuinStar Technology was chosen, with a computed antenna gain of 17.72 dB. The product is a pyramidal horn shape (aperture size of 0.9 by 1.2 in., or 22.8 by 30.5 mm), with square flange and rectangular waveguide WR-12, flange pattern UG-387/U. The price is \$400 based on 1000 units, and is the most expensive component in the receiver. By assuming a higher gain on the transmitting antenna but keeping the transmit power fixed at 750 MW, the following figure was derived:

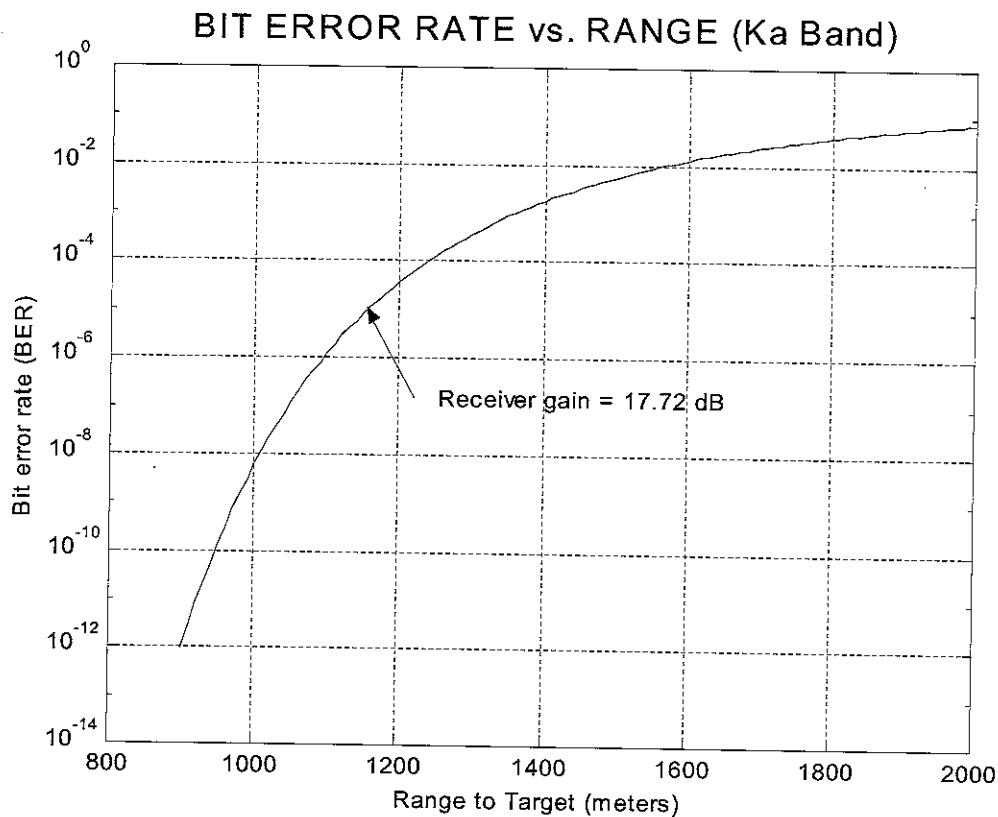


Figure 4. BER Versus Range to Target (m). Transmit Power = 750 MW, $G_t = 65$ dB

D. Error control technique

It is desirable to know whether or not an erroneous command has been generated. However, because of the update rate, there is not enough processing time to perform error correction on the message received. Also, error correction would require a transceiver, that is, the capability to transmit back to the radar. Therefore, a technique was needed for error detection, as opposed to error correction. Note that if an error is detected, it will simply be ignored.

Instead of using a simple parity check code (adding a single bit to the message) that can only detect an odd number of errors, a more robust technique known as CRC will be used for error detection [17]. Strictly speaking, this is a type of block code (distance-4 Bose-Chaudhuri-Hocquenghem code) whose encoder takes a block of finite length, adds redundancy, and creates a word that is longer than the original message. CRC is a widely used technique for error detection in computer networks. With the advent of optical networks and other high-speed data networks in the early 90s, the need for faster CRC algorithms emerged. Consequently, 16-bit and 32-bit parallel CRC architecture were reported in the literature, which are much faster than the serial architecture.

Numerous algorithms for CRC generation have appeared in the literature, showing how optimized Boolean expressions (i.e. digital logic) can be used to represent the CRC in hardware description language [18 through 20]. Prototype VLSI chips have been designed for different communication system applications [21 through 23]. A Programmable Logic Device (PLD) with 24 macrocells “contains enough logic to completely implement the CRC algorithm in parallel” [24]. Therefore, it is recommended that a 16-bit parallel CRC be implemented using Altera’s MAX 7000 EPM7064, a PLD that contains 1250 usable gates and 64 macrocells. This reference also contains Turbo-C code that can be translated into the required PLD equations. Note that the propagation gate delay is between 2.5 and 6 ns, which is a processing time appropriate for this application.

V. DESIGN PRESENTATION

Figure 5 represents the final project design, which began by considering the RF receiver system overview as depicted in Figure 1 [8]. The selection of the horn antenna and chip to implement CRC was discussed in the previous section.

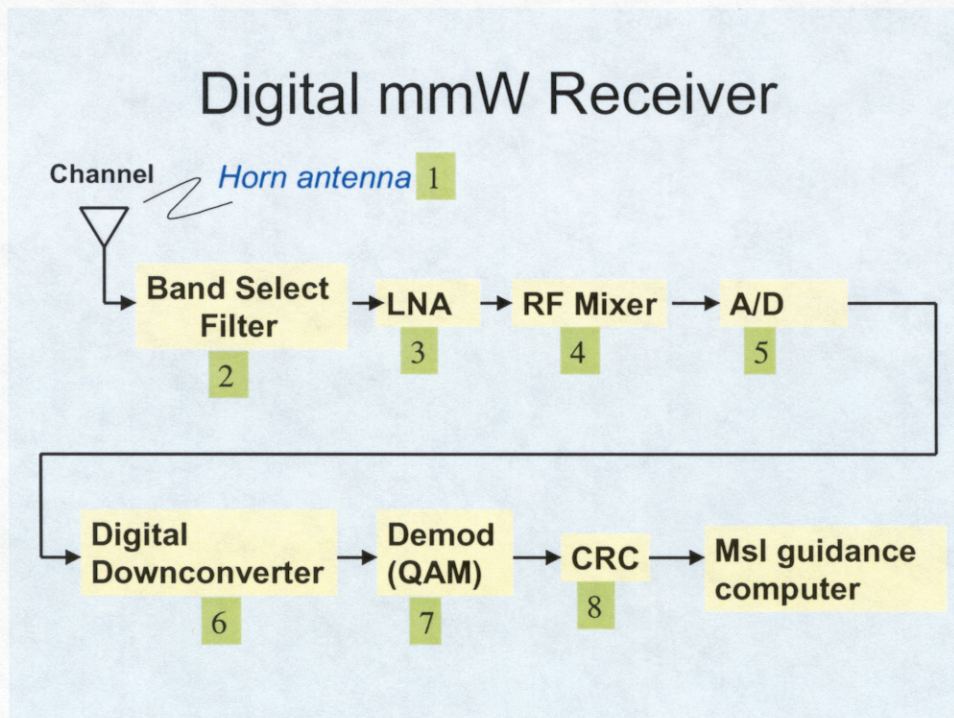


Figure 5. Digital MMW Receiver Design. Numbers Refer to Parts Listing

Merrimac Industries, a company that specializes in interdigital bandpass filters based on their patented "Multi-mix" multilayer fabrication technology, can provide a 35 GHz narrowband filter (5th order Chebyshev) to follow the antenna. The Ka band LNA was chosen from TriQuint Semiconductor based on the performance (gain versus frequency) over a wide frequency range and noise figure. Following the LNA is an RF mixer ("Single Balanced Down Converter") from TriQuint to down convert the 35 GHz signal. Based on Pentek's Wideband Digital Receiver (Model 6216), which is a module that attaches to a DSP processor board, a 12-bit A/D converter from Analog Devices and Graychip's digital down converter was selected (Appendix F).

Broadcom, prominent in the field of cable modems and cable TV set-top boxes, offers several products containing QPSK/QAM chips. The selection of their QAM Receiver Link chip was based on simplicity of architecture. Note that the forward error correction and adaptive decision feedback equalizer will be disabled for this project.

A detailed parts listing that includes vendor, part number, and component size are shown in Table 2.

Table 2. Parts Listing for Millimeter Wave Data Link

Supplier	Item	Part Number/Size	Price
Quinstar Technology	Pyramidal horn antenna	Rectangular waveguide WR-12, flange pattern UG-387/U (Aperture size 22.8 by 30.5 mm)	\$400.00
Merrimac Industries	35 GHz narrowband filter	MMFM-FBGI Interdigital ROC Filter (0.67 by 0.69 by 0.04 in.)	\$20.00
TriQuint Semiconductor	Low noise amplifier	TGA1319C (2.179 by 0.847 mm)	\$30.00
TriQuint Semiconductor	RF mixer	TGC1430E-EPU (1.26 by 1.19 mm)	\$38.00
Analog Devices	12-bit A/D converter	AD6640 (12.0 by 10.0 mm)	\$38.60
Graychip	Digital down converter	GC1012A (32.0 by 28.0 mm)	\$134.00
Broadcom	QAM link receiver	BCM3116 (Size not available without non-disclosure agreement)	\$90.00
Altera	Programmable logic device	EPM 7064: 64 macrocells, 1250 usable gates (0.656 by 0.695 in.)	\$8.40

VI. ATMOSPHERIC EFFECTS ON COMMUNICATION SYSTEMS

A characteristic of all communication systems is that information is transmitted to a receiver by a communication channel or "wave guide". Typical wave-guides are copper wire, fiber optic conduits, or the atmosphere (wireless communications). For an MMW radar communicating to a high velocity missile, the environment influences performance parameters such as detection range and accuracy [6]. The term environment refers to both the electromagnetic energy reflected back to the radar, and the attenuation properties of the atmosphere that lie in the propagation path between the radar and the target. Atmospheric considerations, especially attenuation by rainfall, will be the focus of this discussion.

A. Attenuation by Clear Air

The term "attenuation" refers to the absorption of electromagnetic energy by the medium that lies between the radar transmitter and the receiver. Link budgets for communication systems quantify the amount of attenuation due to environmental factors. In this application, attenuation will prevent guidance commands from reaching the receiver on the missile. In a clear atmosphere where rain, snow, and clouds are absent, there is still some attenuation due to the presence of oxygen and water vapor. For a clear atmosphere containing 1 percent water molecules (7.5 g/m³ of water content), attenuation due to oxygen and water vapor combined is approximately 0.139 dB/km [9].

Note that two peaks due to resonance in the oxygen molecules occur at 60 GHz and 120 GHz, while attenuation due to oxygen slowly decreases below 10 GHz. In the vicinity of 184 GHz, there is a resonance line due to water vapor that severely limits radar operation at this frequency. The oxygen molecule is known to have a permanent dipole moment [25]. The absorption at millimeter wavelengths is due to the magnetic interaction with the incident field resulting in a family of absorption lines. Water vapor has a polar molecule with an electric dipole. The interaction with the incident radiation produces absorption lines in a similar manner. Due to the clear air atmospheric attenuation, most of the radar research and development has taken place at the MMW "windows" of 35 GHz, 95 GHz, 140 GHz, and 220 GHz [6].

B. Attenuation by rainfall

The most important cause of radio link fading in the 10 to 35 GHz frequency range is rain-induced attenuation [26]. The two processes that attenuate MMW energy propagating through rain are absorption and scattering. The absorption and scattering cross-sections refer to the power absorbed and power scattered in all directions by the raindrops when it is radiated by a plane wave of unit power per unit area. Rain-induced attenuation is a function of:

- Frequency
- Temperature
- Raindrop size distributions
- Polarization of the wave. [27]

Most attenuation models are based on the empirical expression

$$\text{Attenuation (dB/km)} = aR^b \quad (3)$$

where R is rainfall rate (mm/hr), and a and b are constants that are primarily functions of frequency.

Noting that “both a and b are mildly sensitive to wave polarization” [9], this discussion will not include the physics of polarization. Instead, an overview of this model will be provided, indicating how these coefficients were derived without giving the theoretical details. This model (Eq. 3) has been adopted by the International Radio Consultative Committee (CCIR), which is the technical advisory body to the International Telecommunications Union (ITU), and will be referred to as the “CCIR Model”. Improvements to the CCIR model and directions for future research will be indicated. Recent experimental measurements and theoretical studies will be cited. Some other rain attenuation models are briefly summarized. The conclusion of this section contains a figure relating BER to target range as a function of rainfall rate based on the CCIR model.

Although the nonlinear relation in Equation (3) was first proposed in 1954 [28], detailed calculations of the coefficients were performed in 1978 [29]. Attenuation values were computed using Mie scattering theory for raindrops at 41 different frequencies. This required the refractive index of water for four different temperatures. Also, since raindrop size distribution is known to differ depending on the type of rainfall, four different drop size distributions were employed. These distributions took into account two approximations for continental temperate rainfall, thunderstorms (large drops), and drizzle (small drops). Logarithmic regression was then applied to the Mie scattering calculations to derive the coefficients (a and b) as a function of frequency. After applying some minor adjustments, the CCIR adopted these coefficients in 1986 [30], indicating both a horizontal and vertical polarization.

A number of improvements have been made to the CCIR model that was adopted in 1986. These improvements are summarized in Table 3. [31]. The term “coordination contour” refers to a closed curve drawn around the planned location of an earth station. This contour refers an interference level derived from propagation models. This approach is quite useful in Europe to indicate where placement of an earth station would result in unacceptable interference levels.

Table 3. Improvements to CCIR – 1986

New CCIR Technique	Factors Included
Transmission Loss Formula	<ul style="list-style-type: none"> • Efficiency of earth-station antenna • Distance from terrestrial station to scattering volume • Frequency (GHz) • Radar reflectivity • Allowance for deviation from Rayleigh scattering law • Attenuation by oxygen and water vapor • Effective scatter transfer function • Considers variation of rain height
Coordination Contour	<ul style="list-style-type: none"> • Distance from maximum scattering to terrestrial station location • Frequency (GHz) • Rain rate exceeded for specified time percentage • Antenna gain of terrestrial station • Allowance for deviation from Rayleigh scattering law

Potential future improvements to the CCIR models include:

- Improved reflectivity factor slope and transmission loss equations
- Improved horizontal structure models for rain cells
- Improved geometry for coordination contours (more realistic terrestrial elevation angles). [31]

Currently there is still a great deal of interest in rain-induced attenuation in the MMW regions. The telecommunication industry continues to evaluate the higher frequency spectrum for transmission of information. In 1999, France Telecom announced a 5-year study to evaluate precipitation effects at 30, 50, 60, and 94 GHz [32] for an 800 m link. This study involves detailed meteorological measurements including rainfall rates, raindrop size distribution, temperature, and wind speed and direction. The Brazilian Center for Telecommunication Studies studied rain attenuation at 15 and 18 GHz [33] based on their assertion that CCIR methods are inaccurate when applied to tropical regions. Their results cannot be directly compared with the CCIR methods since it was concerned with differential attenuation, which is a function of the angle between two data links and their path length difference. The units of differential attenuation are dB, while the CCIR methods specify dB/km.

The justification for including this section is to indicate that numerous models for estimating cumulative attenuation have been developed. A summary of these models is listed in Table 4 [30]. References are included so that the interested reader may pursue further details. Most of these models employ a concept known as “effective path length”, which is equivalent to Equation (3) multiplied by a factor Le :

$$\text{Attenuation} = aR^b Le \quad (4)$$

where Le is the “hypothetical path length of uniform rain rate which will produce the same total path length as the real varying rain rate” [30] along the path.

These models are generally based on climatological data, depicting rain rate or attenuation as the probability of exceedance (abscissa) versus rain rate or attenuation (ordinate). Communication system designers use these models to infer the “outage time”, which is the average length of time a given threshold of rain rate or attenuation is exceeded. The average time between outage periods for a given rain event is also desirable to know.

Table 4. Summary of Rain and Rain Attenuation Models

Model	Inputs	Outputs	Comments
Rice-Holmberg [34]	Climate or site-specific mean annual rainfall plus ratio of thunderstorm to total rain	Cumulative time distribution of rainfall	Two rain modes considered: Thunderstorm and uniform rains. Probability of rain rate exceedance for either or both modes is available.
Dutton-Dougherty [35]	Same as Rice-Holmberg; requires link parameters (e.g. frequency, elevation, and angle)	Rain or gaseous attenuation associated with a given exceedance percentage	Utilizes modified Rice-Holmberg rain model. Provides confidence limits given two additional rain rate distributions
Global [36]	Location and link parameters	Rain associated with a given exceedance percentage	All rain attenuation parameter values are self-contained. Globally applicable.
Two-Component [37]	Same as global.	Exceedance time percentage associated with a given rain attenuation.	Same rain model as for global model. Two rain modes considered: convective cell and debris rains.
CCIR [38]	Same as global.	Rain attenuation associated with a given exceedance time percentage.	All rain attenuation parameter values are self-contained. Globally applicable.
Lin [39]	Five minute rain rate and link parameters.	Attenuation associated with a given rain rate.	Simple extension of terrestrial path rain attenuation model.

C. Attenuation by Clouds, Fog, and Smoke

The approach often cited [9] for attenuation due to fog is based on water content of the cloud or fog (g/m³), and is independent of the drop size distribution. Table 5 summarizes the most common equations for fog attenuation.

Table 5. Attenuation (α : dB/km) Due to Fog

Equation	Comment
$\alpha = 4.867 (10^{-4}) m f^2$ [40]	Coastal fog: $m = 304.1 / V^{1.43}$ Inland fog: $m = 131.9 / V^{1.54}$ • V : Visibility (m) • f : frequency (GHz)
$\alpha = K_c \rho_l$ [38]	ρ_l : liquid water content (g/m ³) K_c : depends on frequency and temperature

Cloud attenuation will not be discussed in detail as the radar-guided missile is expected to fly below most cloud layers. Note that zenith cloud attenuation measurements were taken at 35 GHz, indicating a range of 0.02 to 0.35 dB of attenuation [41].

A thorough analysis of the effect of smoke plumes would require transmittance models of the atmosphere. Without resorting to statistical distributions of smoke particles (which would require complex calculations based on scattering theory) and instead assuming that the presence of smoke lowers visibility, the attenuation in dB/km [9] is

$$\begin{aligned} & 4.867 \cdot 10^{-4} \cdot (304.1) \cdot f_{\text{GHz}}^2 \\ & = 0.19 \text{ dB/km, or } 0.38 \text{ dB one-way for} \\ & (V_m)^{1.43} \end{aligned} \tag{5}$$

a 2 km path. This calculation assumed the equivalent of coastal fog, with a visibility of 120 m. This value is small enough to be ignored for this project. Note that smoke and obscurant data were gathered by military organizations for many years during the "Smoke Week" test programs. Referring to a 1979 test, Knox reported attenuation at 35, 94, and 140 GHz due to red phosphorus smoke over a 600m path [6]. The worst-case attenuation was 0.4 dB.

D. Attenuation by Frozen Hydrometeors

The attenuation caused by frozen hydrometeors in the atmosphere is much less than the attenuation caused by rain at the same precipitation rate. Frozen hydrometeors refer primarily to snow and hail but can also include sleet, snow-sleet mixtures, and ice crystal clouds. There are relatively few studies that discuss attenuation due to snow and hail. In addition, it is difficult to compare results of these studies because of the variation in snowflake size and precipitation fall rate. Snowflakes average between 2 and 5 mm, but can be as large as 15 mm. Snow with high water content can fall 5 to 6 times as fast as dry snow [27]. Wet snow attenuation, however, is comparable to rainfall attenuation in the MMW region.

One of the few studies of snowfall attenuation was made by Hokkaido University of Japan [42]. Measurements were made at 35 GHz, which is the frequency of interest for this report. They found that attenuation (dB/km) was roughly one-half of the precipitation rate (mm/10 min) for wet snow. For example, a precipitation rate of 1.0 mm/10 min corresponded to an attenuation of 2.0 dB/km. The attenuation due to dry snow was only about 0.03 dB/km, which is negligible.

Table 6 summarizes some of the studies relevant to attenuation due to snow, ice crystals, and hail. Note that hail attenuation has been known to impact satellite communications [43]. Also, when ice particles such as hail and sleet begin to melt, these particles can develop a water coating before completely melting. These particles can cause greater attenuation than that due to the all rain layer at lower altitudes.

Table 6. Attenuation (α : dB/km) Due to Snow, Ice Crystals, and Hail

Hydrometeor	Equation or Result	Comment
Snow [29]	$\alpha = 4.568(10^{-8})r^2f^4 + 7.467rf$	r: snowfall rate (mm/hr of melted water content) f: frequency (GHz) Only valid up to 20 GHz
Ice crystals [41]	$\alpha = 1.117(10^{-4})f$	f: frequency (GHz) Attenuation depends on shape of crystals, temperature, and density of ice. Negligible even at high frequencies.
Hail [44]	Measured attenuation in hail falling at 10 mm/hr	Attenuation varied from 0.4 to 2.7 dB/km.

E. Design implications

Figure 6 was computed using the radar range equation and the same assumptions for transmit power, transmit gain, and receiver gain that are indicated for Figure 4. Values for attenuation based on rainfall rates were inferred from the figure, "Attenuation rate (one-way) for rainfall at various frequencies and rainfall rates" [30], which is based on Olsen's calculations [29]. The definition of rainfall rates is:

- Light rain: 2.5 mm/hr
- Medium rain: 12.5 mm/hr
- Heavy rain: 25.0 mm/hr. [45]

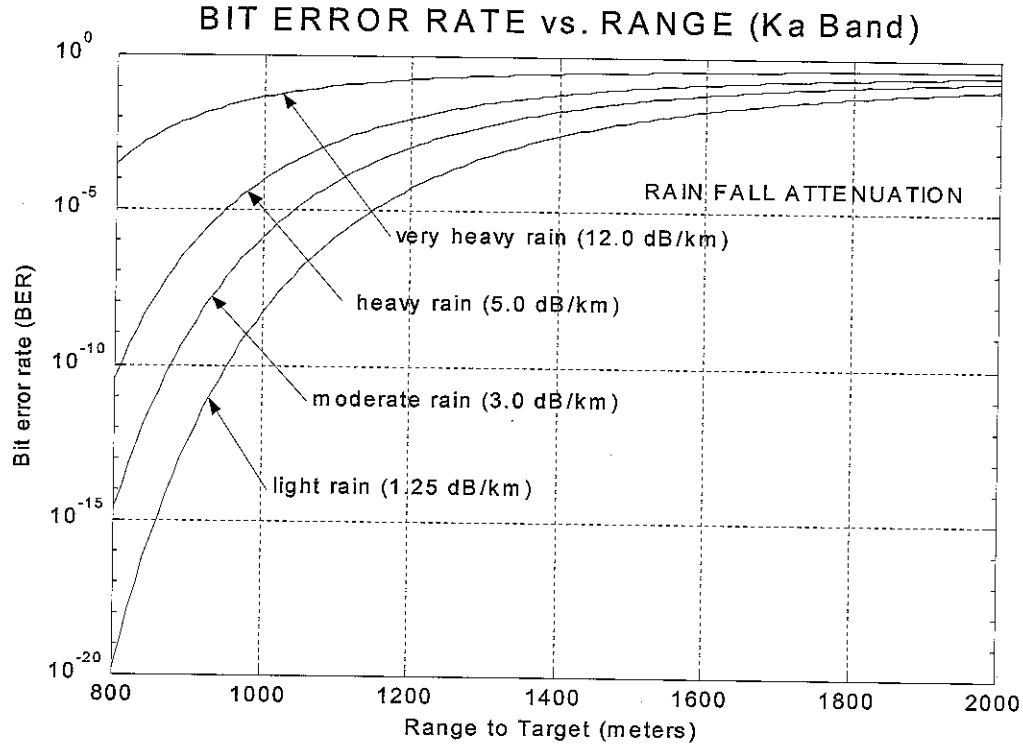


Figure 6. Effect of Rainfall Attenuation on BER Versus Range to Target.
 Transmit Power = 750 mW, $G_t = 65$ dB, $G_r = 17.72$ dB

These computations indicate that a BER of 10^{-6} can still be achieved in a moderate rain, but that the BER increases to more than 10^{-2} for a heavy rain. For the system to work in heavy rain, it is not necessary to re-design the data link. Instead, either the transmit power, transmit gain, or both would have to be increased. It is preferable to increase the transmit gain since increasing the transmit power increases the enemy's chances of detecting the radar system. From Equation (1), the transmit gain is proportional to the area of the transmitter aperture. If the transmitter is mounted on a large vehicle or platform, the transmitter size can be increased provided that size and weight restrictions are not violated.

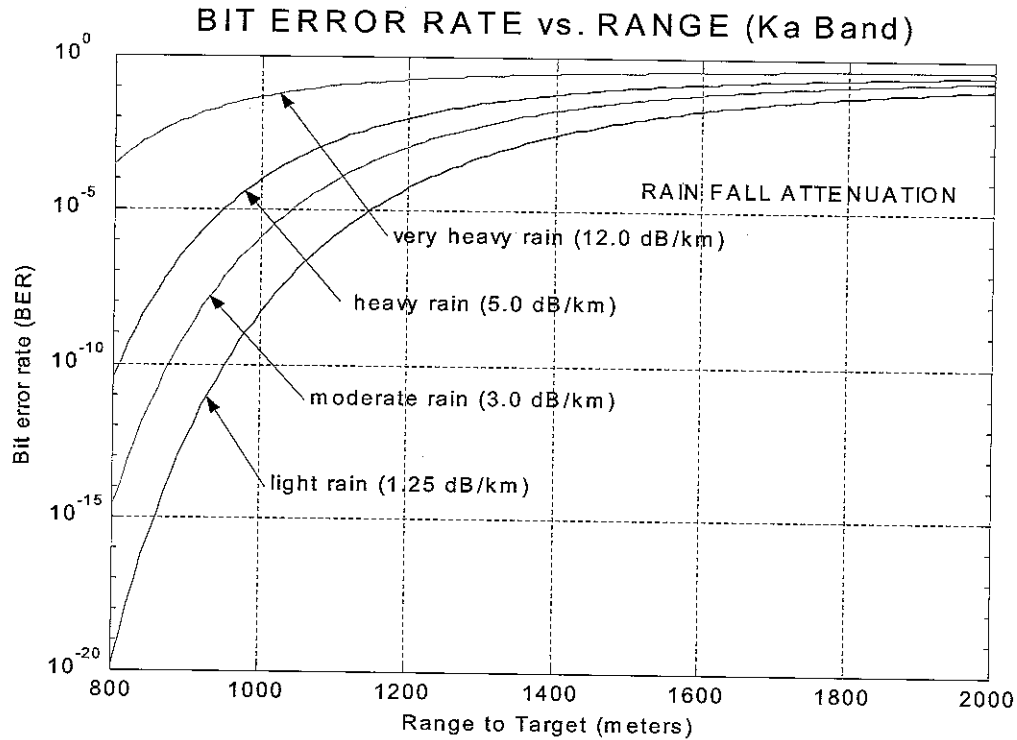


Figure 6. Effect of Rainfall Attenuation on BER Versus Range to Target.
 Transmit Power = 750 MW, $G_t = 65$ dB, $G_r = 17.72$ dB

These computations indicate that a BER of 10^{-6} can still be achieved in a moderate rain, but that the BER increases to more than 10^{-2} for a heavy rain. For the system to work in heavy rain, it is not necessary to re-design the data link. Instead, either the transmit power, transmit gain, or both would have to be increased. It is preferable to increase the transmit gain since increasing the transmit power increases the enemy's chances of detecting the radar system. From Equation (1), the transmit gain is proportional to the area of the transmitter aperture. If the transmitter is mounted on a large vehicle or platform, the transmitter size can be increased provided that size and weight restrictions are not violated.

VII. CONCLUSION

A feasibility study was performed whose objective was a systems-level design of a digital MMW data link capable of receiving a digital data stream (guidance commands) transmitted by a 35 GHz radar. MATLAB was used to simulate the SNR at the MMW data link as the missile travels down range. The simulation verified that the project objective of a BER of 10^{-6} at 1 km downrange was met (radar range equation). Also, the simulation was used to obtain appropriate values for transmitter power and size of the receiver and transmitter apertures. Textbooks and recent journal articles (communication engineering) were then accessed to determine the most efficient modulation scheme. The next phase of the project was the component selection, which was conducted using the Internet search engines Google and IEEE Xplore. These two resources were extremely useful for this phase of the project. Rainfall attenuation was simulated, indicating that a rainfall more intense than a moderate rain would require an increase in transmitter power, larger transmitter aperture, or both to achieve the objective BER.

The project remained on schedule, although significantly more time was spent on the component search than during the initial phases of the project. Reviewing the patent database was helpful in identifying candidate components, particularly those involved in the digital down conversion process. The proposed design cost \$759 (based on 1000 units), which is considerably less than the \$1000 to \$2000 objective price range that appears in the second paragraph of Section II. Although no expensive custom designed chips were required, the design is predicted on the ability to disable some of the features on the QAM demodulator chip, and the implementation of Boolean equations for 16-bit parallel CRC on a programmable logic device.

REFERENCES

1. Federal Communications Commission, "Millimeter Wave Propagation: Spectrum Management Implications," Office of Engineering and Technology, Bulletin 70, July 1997.
2. Heinel, H.H., "Millimeter Wave Technology Since 1985 and Future Trends," IEEE Transactions on Microwave Theory and Devices, 39 (5), 759-767, May 1991.
3. Bruder, J.A., "MMW Low Angle Tracking Radars," In: Currie, N.C.; Brown, C.E., eds., Principles and Applications of Millimeter Wave Radar, Norwood, MA, Artech House, 721-751, 1987.
4. Gentile, Kenneth, "Digital Upconverter IC Tames Complex Modulation," Microwaves and RF, August 2000; <http://www.analog.com>, Accessed January 15, 2001.
5. Digital Receivers Bring DSP to Radio Frequencies, http://www.pentek.com/Tutorials/DR_Radio/DR_Radio.htm, Accessed June 4, 2001.
6. Reedy, E. K., "Fundamentals of MMW Radar Systems," In: Principles and Applications of Millimeter Wave Radar, Currie, N.C.; Brown, C.E., eds., Norwood, MA, Artech House, 19-71, 1987.
7. Eaves, J.L. and Reedy, E.K., eds., Principles of Modern Radar, New York, NY, Van Nostrans, 1987.
8. Stonick, J.T., "RF Communication Systems," Army Research Office Winter School on Digital Communications, San Diego, CA, 1-152, January 2000.
9. Peebles, Peyton Z., Radar Principles, New York, NY: John Wiley, 1998.
10. Das, J., Review of Digital Communications, New York, NY, John Wiley; 1988.
11. Lu, J. [and others], "MPSK and MQAM BER Computation Using Signal-Space Concepts," IEEE Transactions on Communications, 47 (2), 181-184, February 1999.
12. Huang, L.L. and Hanzo, L., "A Recursive Algorithm for the Error Probability Evaluation of MQAM," IEEE Communication Letters, 4 (10), 304-306, October 2000.
13. Albano, R.G. [and others], "Bit Error Performance Evaluation of Double-Differential QPSK in Faded Channels Characterized by Gaussian Plus Impulsive Noise and Doppler Effects," IEEE Transactions on Vehicular Technology, 49 (1), 148-158, January 2000.
14. Beaulieu, N.C. [and others], "Comparison of Four SNR Estimators for QPSK Modulations," IEEE Communication Letters, 4 (2), 43-45, February 2000.
15. Proakis, John G.; Salehi, Masoud, "Contemporary Communication Systems Using MATLAB," Brooks Cole, Pacific Grove, CA, 2000.

REFERENCES (Cont.)

16. Bic, J. C. [and others], Elements of Digital Communication, New York, NY: John Wiley; 1991.
17. Litwin, L. and Ramaswamy, K., "Error Control Coding – An Overview for Modern Coding Techniques in a Digital Communication System," *IEEE Potentials*, 20 (1), 26-31, February 2001.
18. Nair, R. [and others], "A Symbol-Bases Algorithm for Hardware Implementation of Cyclic Redundancy Check (CRC)," *VHDL International Users Forum*, 82-87, 1997.
19. Joshi, S. M. [and others], "A New Parallel Algorithm for CRC Generation," 2000 *IEEE Conference on Communications*, (3), 1764-1768, June 2000.
20. Sodski, A. and Albicki, A., "Parallel Encoder, Decoder, Detector, and Corrector for Cyclic Redundancy Checking," *IEEE International Symposium on Circuits and Systems*, 2945-2948, 1992.
21. Pei, T. and Zukowski, C., "High Speed Parallel CRC Circuits in VLSI," *IEEE Transactions on Communications*, 40 (4), 653-657, April 1992.
22. Thomann, M., "Custom ASIC VLSI Device for Asynchronous Transfer Mode, *IEEE International Solid State Circuits Conference*, Session 7: Paper FA 7.1, 114-116, 1996.
23. Li, S.H. and Zukowski, C., "A Self-Timed Cyclic Redundancy Check (CRC) in VLSI," *Proceedings of the 40th Midwest Symposium on Circuits and Systems*, (2):1021-1023, Sacramento, CA, August 1997.
24. Ganssle, J.G., *Computing CRCs in Parallel*. 1991,
<http://www.hmi.com/company/articles/magazine/acrc.htm>, Accessed March 15, 2001.
25. Verma, A.K. [and others], "Effect of the Atmosphere on Radio and Radar Performance," *Fourth IEEE Region 10 International Conference*, 844-847, November 1989.
26. Stutzman, W.L. and Yon, K.M., "A Simple Rain Attenuation Model for Earth-Space Radio Links Operating at 10-35 GHz," *Radio Science*, 21 (1), 65-72, February 1986.
27. Trebits, R.N., "MMW Propagation Phenomena," In: Currie, N.C.; Brown, C.E., eds. Principles and Applications of Millimeter Wave Radar, 131-188, Norwood, MA: Artech House, 1987.
28. Gunn, K.L.S. and East, T.W.R., "The Microwave Properties of Precipitation Particles," *Quarterly Journal of the Royal Meteorological Society*, 80, 522-545, October 1954.

REFERENCES (Cont.)

29. Olsen, Robert L. [and others], "The aR^b Relation in the Calculation of Rain Attenuation," IEEE Transactions on Antennas and Propagation, AP-2 (2), 318-329, March 1978.
30. Ippolito, L. J., "Propagation Effects Handbook for Satellite System Design," NASA Reference Publication 1082 (4), February 1989
31. Olsen, Robert L. [and others], "Interference Due to Hydrometeor Scatter on Satellite Communication Links," Proceedings of the IEEE, 81 (6), 914-922, June 1993.
32. Veyrunes, O. [and others], "First Results of Precipitation Effects at 30, 50, 60, and 94 GHz on an 800m Link in Belfort (France)," IEE National Conference on Antennas and Propagation, 77-80, April 1999.
33. Mello, L. S. [and others], "Measurements of Rain Attenuation in 15 and 18 GHz Converging Links," Ninth International Conference on Antennas and Propagation, 127-130, April 1995.
34. Rice, P. L. and Holmberg, R.N., "Cumulative Time Statistics of Surface Point Rainfall Rates," IEEE Transactions on Communications, COM-21 (10), 1131-1136, 1973.
35. Dutton, E. J. [and others], "An Improved Model for earth-Space Microwave Attenuation Distribution Prediction," Radio Science, 17 (6), 1360-1370, 1982.
36. Crane, Richard K., "Prediction of Attenuation by Rain," IEEE Transactions on Communications, COM-28 (9), 1717-1733, 1980.
37. Crane, Richard K., "A Two-Component Rain Model for the Prediction of Attenuation Statistics," Radio Science, 17 (6), 1371-1387, 1982.
38. International Radio Consultative Committee, "Propagation Data and Prediction Methods Required for Earth-Space Telecommunication Systems," Report 564-3 in Volume V, Recommendations and Reports of the CCIR-1986, Geneva, Switzerland: International Telecommunications Union, 1986.
39. Lin, S. H. [and others], "Rain Attenuation on Earth-Satellite Paths – Summary of 10-Year Experiments and Studies," Bell Systems Technical Journal, 59 (2), 183-228, 1980.
40. Kerr, D. E., Propagation of Short Radio Waves, Lexington, MA: Boston Technical Publishers, 1964.
41. Lo, L. I. [and others], "Attenuation of 8.6 and 3.2 mm Radio Waves by Clouds," IEEE Transactions in Antennas and Propagation, AP-2 (6), 1-5, 1975.

REFERENCES (Conc.)

42. Nishitsuji, A. and Matsumoto, A., "Calculation of Radio Wave Attenuation Due to Snowfall," Monograph of the Research Institute of Applied Electricity, Hokkaido University, (19), 63-78, 1971.
43. Anatar, Y. M. M. and Hendry, A., "Attenuation of Radio Waves by Atmospheric Wet Ice and Mixed Phase Hydrometeors," Proceedings of the URSI Commission F, Louvain, Belgium, 455-461, 1983.
44. Aganbekyan [and others], "The Propagation of Submillimeter, Infrared, and Visible Waves in the Earth's Atmosphere," Rasprostraneniye Radiovoln, Institut Radiotekhniki I Electroniki, 187-227, 1975.
45. Hudson, R. F., Infrared System Engineering, New York, NY: John Wiley; 1969.

BIBLIOGRAPHY

- Aganbekyan [and others]. The propagation of submillimeter, infrared, and visible waves in the earth's atmosphere. Rasprostraneniye Radiovoln, Institut Radiotekhniki I Electroniki. 1975; 187-227.
- Albano, R.G. [and others]. Bit error performance evaluation of double-differential QPSK in faded channels characterized by Gaussian plus impulsive noise and Doppler effects. IEEE Transactions on Vehicular Technology. 2000 January; 49 (1): 148-158.
- Anatar, Y.M.M.; Hendry, A. Attenuation of radio waves by atmospheric wet ice and mixed phase hydrometeors. Proceedings of the URSI Commission F; 1983; Louvain, Belgium: 455-461.
- Beaulieu, N.C. [and others]. Comparison of four SNR estimators for QPSK modulations. IEEE Communication Letters. 2000 February; 4 (2):43-45.
- Bic, J.C. [and others]. Elements of digital communication. New York, NY: John Wiley; 1991.
- Bruder, J.A. MMW low angle tracking radars. In: Currie, N.C.; Brown, C.E., eds. Principles and applications of millimeter wave radar. Norwood, MA: Artech House; 1987: 721-751.
- Buss, John Michael [and others]. Hybrid instruction set for versatile digital signal processing system. Unites States Patent 5,852,730. 1998 December 22; 1-20.
- Crane, Richard K. Prediction of attenuation by rain. IEEE Transactions on Communications. 1980; COM-28 (9): 1717-1733.
- Crane, Richard K. A two-component rain model for the prediction of attenuation statistics. Radio Science. 1982; 17 (6): 1371-1387.
- Crane, Richard K. Propagation modeling – past, present, and future. International Conference on Antennas and Propagation. 1989; (2): 263-267.
- Crane, Richard K.; Robinson, Paul C. ACTS propagation experiment: rain-rate distribution observations and prediction model comparisons. Proceedings of the IEEE. 1997 June; 85(6): 946-958.
- Das, J. Review of digital communications. New York, NY: John Wiley; 1988.
- Digital receivers bring DSP to radio frequencies. http://www.pentek.com/Tutorials/DR_Radio/DR_Radio.htm. Accessed June 4, 2001.
- Dutton, E.J. [and others]. An improved model for earth-space microwave attenuation distribution prediction. Radio Science. 1982; 17 (6):1360-1370.
- Eaves, J.L.; Reedy, E.K., eds. Principles of modern radar. New York, NY: Van Nostrans; 1987.

BIBLIOGRAPHY (Cont.)

- Federal Communications Commission. Millimeter wave propagation: spectrum management implications. Office of Engineering and Technology. 1997 July; Bulletin 70.
- Fox, James G. [and others]. Sine/cosine generator and method. United States Patent RE36,388. 1999 November 9; 1-23.
- Ganssle, J.G. Computing CRCs in parallel. 1991;
<http://www.hmi.com/company/articles/magazine/acrc.htm>. Accessed March 15, 2001.
- Gentile, Kenneth. Digital upconverter IC tames complex modulation. Microwaves and RF. 2000 August; <http://www.analog.com>. Accessed January 15, 2001.
- Gunn, K.L.S.; East, T.W.R. The microwave properties of precipitation particles. Quarterly Journal of the Royal Meteorological Society. 1954 October; 80: 522-545.
- Heinel, H.H. Millimeter wave technology since 1985 and future trends. IEEE Transactions on Microwave Theory and Devices. 1991 May; 39 (5): 759-767.
- Huang, L.L.; Hanzo, L. A recursive algorithm for the error probability evaluation of MQAM. IEEE Communication Letters. 2000 October; 4 (10): 304-306.
- Hudson, R.F. Infrared system engineering. New York, NY: John Wiley; 1969.
- International Radio Consultative Committee. Propagation data and prediction methods required for earth-space telecommunication systems. Report 564-3 in Volume V, Recommendations and Reports of the CCIR-1986. Geneva, Switzerland: International Telecommunications Union; 1986.
- Ippolito, L.J. Propagation effects handbook for satellite system design. NASA Reference Publication 1082 (4); 1989 February.
- Joshi, S.M. [and others]. A new parallel algorithm for CRC generation. 2000 IEEE Conference on Communications. 2000 June; (3):1764-1768.
- Kerr, D.E. Propagation of short radio waves. Lexington, MA: Boston Technical Publishers; 1964.
- Li, J. [and others]. A six-port direct digital millimeter wave receiver. IEEE MTT-S International. 1994 May; 3:1659-1662.
- Li, S.H.; Zukowski, C. A self-timed cyclic redundancy check (CRC) in VLSI. Proceedings of the 40th Midwest Symposium on Circuits and Systems, Sacramento, CA. 1997 August; (2):1021-1023.
- Li, Wenzhen [and others]. Ka-Band land mobile satellite channel model incorporating weather effects. IEEE Communication Letters. 2001 May; 5 (5): 194-196.

BIBLIOGRAPHY (Cont.)

- Lin, S.H. [and others]. Rain attenuation on earth-satellite paths – summary of 10-year experiments and studies. *Bell Systems Technical Journal*. 1980; 59 (2): 183-228.
- Ling, C.C.; Reibiz, G.M. A 94 GHz planar monopulse tracking receiver. *IEEE Transactions on Microwave Theory and Techniques*. 1994 October; 42 (10):385-388.
- Litwin, L.; Ramaswamy, K. Error control coding – an overview for modern coding techniques in a digital communication system. *IEEE Potentials*. 2001 February; 20 (1): 26-31.
- Livieratos, P.N. [and others]. Availability and performance of satellite links suffering from interference by an adjacent satellite and rain feeds. *IEE Proceedings – Communications*. 1999 February; 146 (1): 61-67.
- Lo, L.I. [and others]. Attenuation of 8.6 and 3.2 mm radio waves by clouds. *IEEE Transactions in Antennas and Propagation*. 1975; AP-2 (6): 1-5.
- Lu, J. [and others]. MPSK and MQAM BER computation using signal-space concepts. *IEEE Transactions on Communications*. 1999 February; 47 (2): 181-184.
- Mello, L.S. [and others]. Measurements of rain attenuation in 15 and 18 GHz converging links. *Ninth International Conference on Antennas and Propagation*. 1995 April; 2:127-130.
- Nair, R. [and others]. A symbol-bases algorithm for hardware implementation of cyclic redundancy check (CRC). *VHDL International Users Forum*. 1997; 82-87.
- Nathanson, Harvey C. [and others]. Monolithic microwave integrated circuit on high resistivity silicon. *United States Patent 5,449,953*. 1995 September 12; 1-10.
- Nishitsuji, A.; Matsumato, A. Calculation of radio wave attenuation due to snowfall. *Monograph of the Research Institute of Applied Electricity, Hokkaido University*. 1971; (19): 63-78.
- Olsen, Robert L. [and others]. The aR^b relation in the calculation of rain attenuation. *IEEE Transactions on Antennas and Propagation*. 1978 March; AP-2 (2): 318-329.
- Olsen, Robert L. [and others]. Interference due to hydrometeor scatter on satellite communication links. *Proceedings of the IEEE*. 1993 June; 81 (6): 914-922.
- Otung, I.E. [and others]. Rain attenuation statistics of Ka-band earth-space path. *Ninth International Conference on Antennas and Propagation*. 1995 April; 2: 85-88.
- Paoletta, Arthur. Method of making a millimeter wave monolithic integrated circuit. *United States Patent 4,861,426*. 1989 August 29; 1-5.
- Peebles, Peyton Z. *Radar principles*. New York, NY: John Wiley; 1998.

BIBLIOGRAPHY (Conc.)

- Proakis, John G.; Salehi, Masoud. Contemporary communication systems using MATLAB. Pacific Grove, CA: Brooks Cole; 2000.
- Pei, T.; Zukowski, C. High speed parallel CRC circuits in VLSI. IEEE Transactions on Communications. 1992 April; 40 (4): 653-657.
- Reedy, E.K. Fundamentals of MMW radar systems. In: Principles and applications of millimeter wave radar. Currie, N.C.; Brown, C.E., eds. Norwood, MA: Artech House; 1987:19-71.
- Rice, P.L.; Holmberg, R.N. Cumulative time statistics of surface point rainfall rates. IEEE Transactions on Communications. 1973; COM-21 (10): 1131-1136.
- Sodski, A.; Albicki, A. Parallel encoder, decoder, detector, and corrector for cyclic redundancy checking. IEEE International Symposium on Circuits and Systems. 1992; 2945-2948.
- Stonick, J.T. RF communication systems. Army Research Office Winter School on Digital Communications, San Diego, CA. 2000 January; 1-152.
- Stutzman, W.L.; Yon, K.M. A simple rain attenuation model for earth-space radio links operating at 10-35 GHz. Radio Science. 1986 February; 21 (1):65-72.
- Thomann, M. Custom ASIC VLSI device for asynchronous transfer mode. IEEE International Solid State Circuits Conference. 1996; Session 7: Paper FA 7.1, 114-116.
- Trebits, R.N. MMW propagation phenomena. In: Currie, N.C.; Brown, C.E., eds. Principles and applications of millimeter wave radar. Norwood, MA: Artech House; 1987: 131-188.
- Verma, A.K. [and others]. Effect of the atmosphere on radio and radar performance. Fourth IEEE Region 10 International Conference. 1989 November; 844-847.
- Veyrunes, O. [and others]. First results of precipitation effects at 30, 50, 60, and 94 GHz on an 800m link in Belfort (France). IEE National Conference on Antennas and Propagation. 1999 April; 77-80.
- Young, William R.; Chester, David B. Digital down converter and method. United States Patent Office 5,493,581. 1996 February 20; 1-23.
- Young, William R.; Chester, David B. Phase generator. United States Patent 5,570,392. 1996 October 29; 1-28.

APPENDIX A
MARKET RESEARCH

APPENDIX A MARKET RESEARCH

- There are few reports of digital MMW receivers in the literature. Those that are reported are experimental in nature (1:1659-1662).
- There are no patents assigned to "digital MMW receiver"
- There is an emerging market for MMW devices for wireless communication networks. Also, there is a market for MMW sensors that have industrial application (to control processes) and automotive applications. Developments in digital receiver architectures may lead to improvements in these sensors.
- There is considerable research on components such as High Electron Mobility Transistors (HEMT) for use in circuits that implement receiver architectures on a semiconductor wafer (i.e. on a chip). A patent appeared in 1989 entitled, "Method of making a millimeter wave monolithic integrated circuit" (A. Paoella). This method outlines a methodology for developing circuits that can be used as oscillators and amplifiers in the microwave and millimeter wave region. A 94 GHz monopulse tracking receiver that can be implemented on a chip was reported in 1994 (2:385-388).
- There does not appear to be any company offering a complete package that could be purchased off-the-shelf to meet the objectives of the project. However, there are numerous companies that offer components that can potentially be used in the systems design. For example, Graychip, Inc. offers digital filters, digital tuners, QAM modem chipsets, and other digital signal processing (DSP) chips and systems. Wideband Computers, Inc. and Drake Digital also feature QAM systems. Analog Devices, Inc. develops digital upconverters for RF interfaces, including digital filters and other DSP functions integrated on a single chip. TriQuint Semiconductor has numerous low noise amplifiers (LNA) based on HEMT technology integrated on a small chip (several mm²). While there are companies such as Coryell and Wiprud, Inc. that offer custom design of digital receivers, digital transmitters, demodulators, etc, ARCOM Inc. appears to be unique due to its focus on MMW products primarily for wireless communication networks. ARCOM uses and reuses MMIC components for custom design of MMW transceivers, and produces components for digital radios varying from FSK to QAM systems (They note that the trend is towards higher-level QAM systems). Their product matrix (LNAs, up/down converters, etc.) span various bands between 13 and 60 GHz.

APPENDIX B
PATENT SEARCH

APPENDIX B PATENT SEARCH

Table B-1. Patent search on "Digital Receiver Chip"

Patent No.	Date	Title
RE36,388	NOV 99	Sine/cosine generator and method
5,852,730	NOV 98	Hybrid instruction set for versatile digital signal processing system
5,570,392	OCT 96	Phase generator
5,493,581	FEB 96	Digital down converter and method
4,449,953	SEP 95	Monolithic microwave integrated circuit on high resistivity silicon

Some additional details concerning "Digital down converter and method" (cited above) are provided on the following page.

Young, William R.; Chester, David B. Digital down converter and method. United States Patent 5,493,581. 1996 February 20; 5-6.

A digital down converter for extracting a signal from a complex digital signal wherein the real and imaginary components of the complex digital signal are each modulated to shift the center frequency of the desired signal to zero frequency, decimated digitally to limit the bandwidth of each to the bandwidth of the desired signal and filtered to alter the shape thereof. The digital down converter includes a formatter for arranging the output of the desired signal in one of multiple output formats and a controller for programmably controlling the modulation, decimation and filtering and for selecting the desired output format.

The present invention relates to electronic devices, and, more particularly, to semiconductor circuits and methods useful for extracting sub band information from broadband digital data streams.

Communications systems such broadcast radio use frequency division multiplexing (FDM) to simultaneously transmit differing information signals from several sources in a single locale. Typically, each source modulates its carrier frequency with its information signal and keeps within its allocated frequency band. Extraction of a desired information signal from a received broadband of simultaneous broadcasts may be performed by mixing down (down conversion by the selected carrier frequency) followed by low pass filtering and demodulation. Indeed, system 100 receives radio frequency signals (e.g., 100-200 MHz) at antenna 102, filters and mixes the signals down to intermediate frequencies (e.g., 1-10 MHz) with a wideband tuner 104, converts from analog to digital format with sampling analog-to-digital converter 106, extracts the selected frequency band (e.g., of width 5 KHz) with digital down converter 108 which performs the down conversion and filtering, and demodulates and reconstructs an analog information signal with demodulator/processor 110. For example, if wideband tuner 104 has a 10 MHz output bandwidth, then analog-to-digital converter 106 will sample at 20 MHz or more (at least the Nyquist rate), and digital down converter 108 will output a 5 KHz selected band at a

sampling rate of 10 KHz. That is, digital down converter 108 may decrease the sampling rate due to the small bandwidth of its output without loss of information.

The problems of construction of system 100 include realizing digital down converter 108 operating at a high sampling frequency while maintaining a low ripple sharp cutoff filter which has programmable down conversion frequency and programmable bandwidth. Known realizations of a down conversion function include the combination of a numerically controlled oscillator/modulator (NCOM) such as the HSP45106 manufactured by Harris Corporation together with two decimating digital filters (one for the in-phase and one for the quadrature outputs of the NCOM) such as the HSP43220 also manufactured by Harris Corporation. A single chip realization such as the **GC1011 digital receiver chip manufactured by Graychip, Inc.**

APPENDIX C
LOGARITHMIC FORM OF THE RADAR RANGE EQUATION

APPENDIX C
LOGARITHMIC FORM OF THE RADAR RANGE EQUATION

$$\text{SNR (dB)} = P_t + G_t + G_r + 2*\lambda + \sigma - 4*R - B - F_n - L + 71$$

P_t : transmitter power (dBW)

G_t : antenna gain, transmitter (dB)

G_r : antenna gain, receiver (dB)

λ : wavelength (cm)

σ : radar cross section (dB(m²))

R : range (dBm)

B : update rate (dBMHz)

F_n : noise figure

L : losses (dB)

APPENDIX D
BER VERSUS RANGE FOR 4 QAM, 16 QAM, AND 64 QAM

APPENDIX D
BER VERSUS RANGE FOR 4 QAM, 16 QAM, AND 64 QAM
BIT ERROR RATE vs. RANGE (Ka Band)

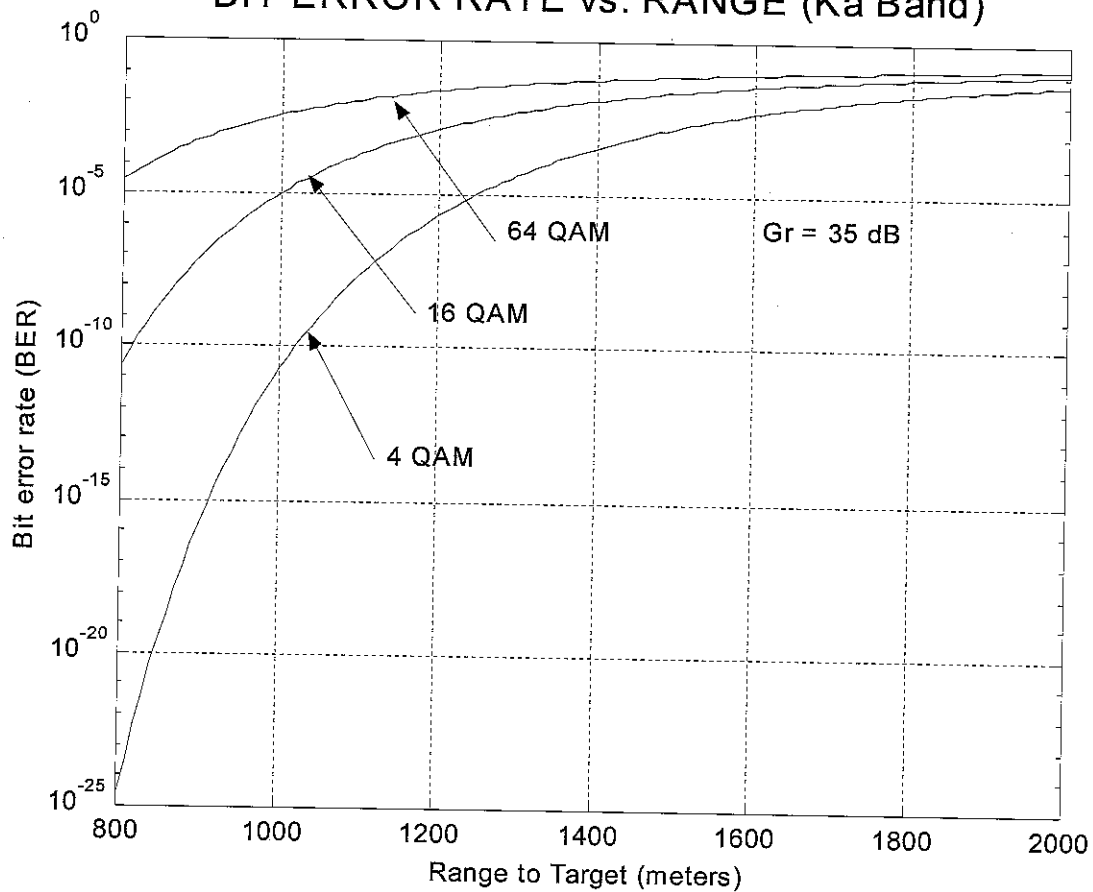


Figure D-1. BER Versus Range to Target for Different Modulations

Table D-1. Conversion of SNR to BER for Different Modulations.

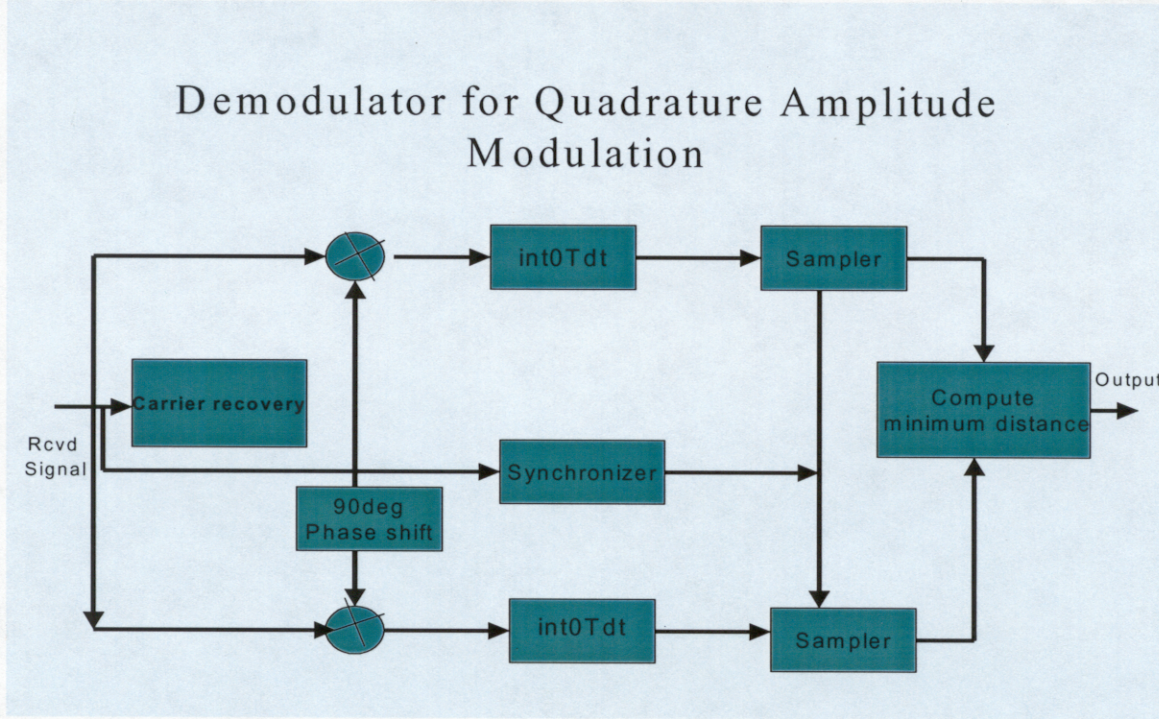
Modulation Name	BER
QPSK (4QAM)	$1/2 * \text{erfc}(\sqrt{E_b/N_0})$
8PSK	$1/3 * \text{erfc}(\sqrt{E_b/N_0 * 3 * \sin(2\pi/8)})$
16PSK	$1/4 * \text{erfc}(\sqrt{E_b/N_0 * 4 * \sin(2\pi/16)})$
16QASK (16QAM)	$3/8 * \text{erfc}(\sqrt{2/5 * E_b/N_0})$
64QASK (64QAM)	$7/24 * \text{erfc}(\sqrt{1/7 * E_b/N_0})$

(3:176-182)

APPENDIX E

QAM DEMODULATOR

APPENDIX E QAM DEMODULATOR



(4:312)

Fig. E-1. Demodulation and Detection of QAM Signals

Broadly speaking, quadrature amplitude modulation (QAM) is a hybrid technique, combining digital amplitude and digital phase modulation. The transmitted QAM signal waveforms are

$$U_{mn}(t) = A_{mc}g_T(t)\cos(2\pi f_c t + \mu_n) \quad m=1,2, \dots, M_1 \quad n=1,2, \dots, M_2$$

QAM results in the simultaneous transmission of $K_1 + K_2 = \log_2 M_1 M_2$ bits occurring at a symbol rate $R_b/(K_1 + K_2)$, if $M_1 = 2^{K_1}$ and $M_2 = 2^{K_2}$.

For demodulation, considering the phase offset p introduced during the signal transmission and the corruption by additive Gaussian noise, the received signal may be expressed as

$$R(t) = A_{mc}g_T(t)\cos(2\pi f_c t + \phi) + A_{ms}g_T(t)\sin(2\pi f_c t + \phi) + n(t), \text{ where}$$

$$n(t) = n_c(t)\cos 2\pi f_c t - n_s(t)\sin 2\pi f_c t$$

The received signal is correlated with the two phase-shifted basis functions:

$$\phi_1(t) = g_T(t)\cos(2\pi f_c t + \phi)$$

$$\phi_2(t) = g_T(t)\sin(2\pi f_c t + \phi)$$

The correlator outputs are sampled and sent to the detector. The purpose of the phase locked loop (used for carrier recovery) is to estimate the carrier phase offset p of the received signal and then phase shift ϕ_1 and ϕ_2 . The clock is synchronized to the received signal to ensure that the correlator outputs are sampled at the appropriate time. The two correlator outputs are:

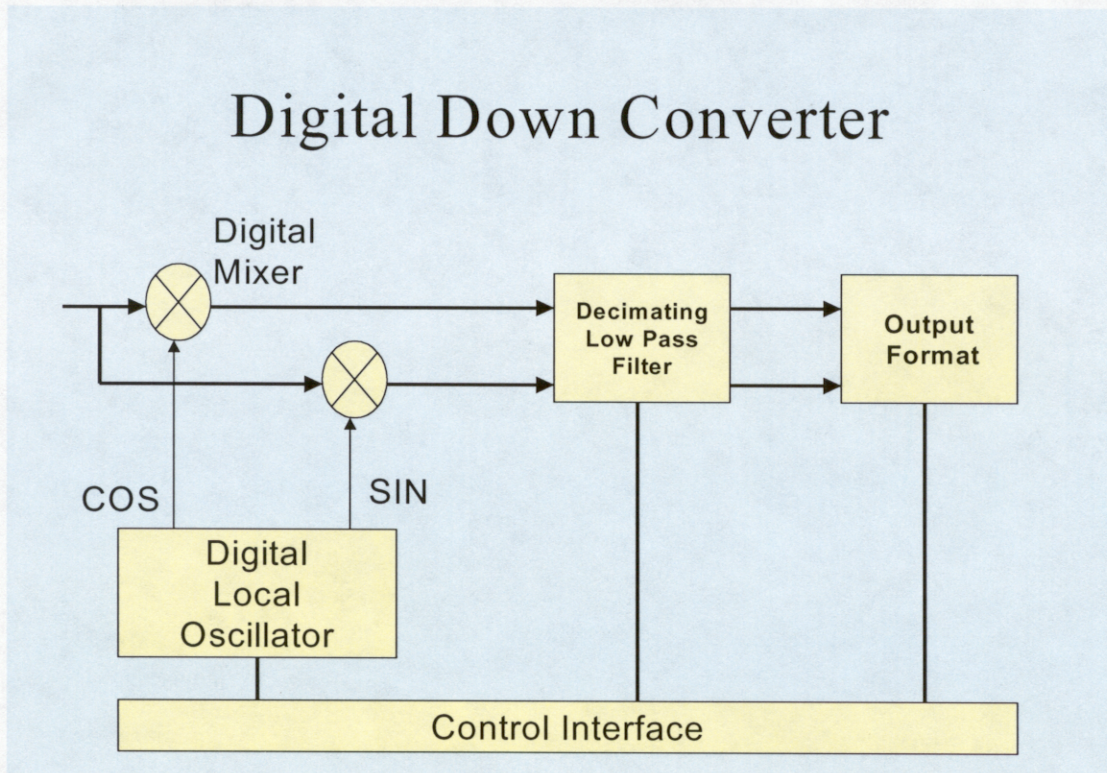
$$R_c = A_{mc} + n_c \cos \phi - n_s \sin \phi$$

The noise components n_s and n_c are uncorrelated Gaussian random variables (zero mean, variance $N_0/2$).

The detector then computes the distance metrics.

APPENDIX F
DIGITAL DOWN CONVERTER

APPENDIX F
DIGITAL DOWN CONVERTER



(5:3)

Figure F-1. Digital Down Converter

APPENDIX G
REFERENCE LIST

APPENDIX G

REFERENCE LIST

1. Li, J. [and others]. A six-port direct digital millimeter wave receiver. *IEEE MTT-S International*. 1994 May; 3:1659-1662.
2. Ling, C.C.; Reibiz, G.M. A 94 GHz planar monopulse tracking receiver. *IEEE Transactions on Microwave Theory and Techniques*. 1994 October; 42 (10):385-388.
3. Bic, J.C. [and others]. *Elements of digital communication*. New York, NY: John Wiley; 1991.
4. Proakis, John G.; Salehi, Masoud. *Contemporary communication systems using MATLAB*. Pacific Grove, CA: Brooks Cole; 2000.
5. Digital receivers bring DSP to radio frequencies. http://www.pentek.com/Tutorials/DR_Radio/DR_Radio.htm Accessed June 4, 2001.

INITIAL DISTRIBUTION LIST

	<u>Copies</u>
IIT Research Institute ATTN: GACIAC 10W. 35th Street Chicago, IL 60616	1
Defense Technical Information Center 8725 John J. Kingman Rd., Suite 0944 Ft. Belvoir, VA 22060-6218	1
AMSAM-RD, Ellen Mahathey	1
AMSAM-RD-AS-AC-CL, Larry Levitt	10
AMSAM-RD-AS-I-RSIC	2
AMSAM-RD-AS-I-TP	1
AMSAM-RD-AS-TI, Buddy Thomas	1
AMSAM-L-G-I, Fred Bush	1